www.czasopisma.pan.pl PAN www.journals.pan.pl
POLSKA AKADEMIA NAUK

jet INTL JOURNAL OF ELECTRONICS AND TELECOMMUNICATIONS, 2020, VOL. 66, NO. 1, PP. 37-43
Manuscript received November 16, 2019; revised January, 2020. DOI: 10.24425/ijet.2019.130263

Design of Millimeter-Wave Six-Port Device for LTCC Technology

Słojewska Barbara, Yashchyshyn Yevhen

Abstract—In this paper a design of millimeter-wave six-port device for LTCC (Low Temperature Cofired Ceramic) technology is presented. Furthermore, problems with implementation of the project taking into account requirements of LTCC technology are discussed.

Keywords—Low Temperature Cofired Ceramic, LTCC, microwave technology, millimeter-wave, six-port network

I. Introduction

NOWADAYS, there is hard to imagine life without the Internet. We are creating 2.5 quintillion bytes of data every day and it is accelerating with the growth of the Internet of Things (IoT). Lower frequency bands (below 6 GHz) are highly occupied. For this reason millimetre-wave (mm-wave) range is increasingly used for data transmission. One of the most commonly used frequencies are from 24 GHz to 24.25 GHz and it is so called industrial, scientific and medical (ISM) band. This is unlicensed band, so it is used in many applications, e.g., short-range radar technology or in radiocommunication systems because wider bandwidth is related to the higher bitrate.

Designing structures for higher frequencies is very challenging and related to many difficulties. Moreover, some technological aspects have to be taken into account. First of all, shorter wavelength resulting smaller dimensions of the structure increases the requirements of fabrication accuracy, resolution (even of the order of micrometres) and reproducibility. In the case of mm-wave devices small change of the geometry may lead to significant deterioration of their parameters. As a consequence, mechanical and temperature stability is also very important.

Another issue is the choice of appropriate substrate. FR4, the most popular laminate used in printed circuit board (PCB), at higher frequencies has too high losses. Therefore, using special microwave substrates is necessary. Due to the small thickness of substrates which are used in mm-wave range, they often require some additional layer (e.g., alumina plate) to make whole structure more durable. There are a few technologies meeting requirements for higher frequencies. One of them is Low Temperature Co-fired Ceramic (LTCC) which is multilayer technology [1]. It has many advantages, such as good high-frequency characteristics, mechanical strength and temperature stability. While using special zero shrinkage LTCC foils there is a low shrinkage in X and Y directions having higher shrinkage than in other LTCC ceramics in Z direction [2]. In many cases shrinkage in Z direction have a low impact on structure parameters compared to other directions. LTCC technology can be used to make various structures, for example, filters, couplers or antennas, working at higher frequencies, such as 60 GHz or 94 GHz.

Barbara Słojewska and Yevhen Yashchyshyn are with Warsaw University of Technology, Institute of Radioelectronics and Multimedia Technology (e-mail: B.Slojewska@stud.elka.pw.edu.pl, E.Jaszczyszyn@ire.pw.edu.pl).

In this paper a design of millimeter-wave six-port device for low shrinkage LTCC technology is presented. Six-port is a passive device which consists of three couplers and one power divider [3]. It has two input ports and four output ports. Output signals are superposition of input signals, which are superimposed under four different relative phase shifts. These static phase shifts between input signals for particular outputs are equal to 0°, 90°, 180°, and 270°, respectively [4]. The block diagram of the designed structure is shown in Fig. 1. Six-ports have many different applications. In microwave metrology they can be utilized as a reflectometers. Second application of six-ports is communication receiver for which the modulated in-phase and quadrature (I/Q) signals can be determined. Six-ports can also be used in a direction of arrival (DoA) measurement system. The angle of incoming signal is obtained based on measured power levels after simple post-processing [5].

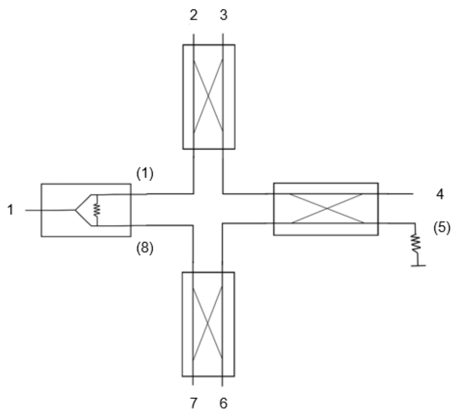

Fig. 1. The block diagram of the designed six-port

Summarizing, it can be stated that there are two biggest advantages of six-ports. They are passive devices and they have phase measurement capability.

II. Design General Statement

The LTCC technology allows to design multilayer structures and enables to reduce the overall surface of a device. It is possible by adding layers in the volume of the structure and by making interconnections between particular layers.

There are two ways to design that six-port – using stripline or microstrip. Microstrip version would be simpler for fabrication, including mounting connectors and discrete components (e.g., resistors). In the case of stripline structure, components such as resistors have to be buried between layers. It complicates technological process. However, it provides possibility to create multilayer structures. Therefore, the usage of stripline is more flexible and allows to place parts of the structure above or under other parts [6].

To sum up, microstrip structure is easier to fabricate but only using stripline allows to create multilayer structures. Taking into account arguments mentioned above, it was decided to design microstrip power divider and stripline couplers. To simplify mounting connectors, microstrip lines have to be added to stripline ports.

III. Design of Six-Port Device by Using of Quasi-Static Simulator

In the beginning, the six-port device was designed by using NI AWR Design Environment. The stripline was intended to be use for all parts of the six-port. It was assumed that zero shrinkage LTCC foils ESL 41110-T will be used. Electrical parameters of this material were measured at Warsaw University of Technology [7]. Therefore, in simulation models of the structure it was assumed that relative permittivity equals to 4.05 and the thickness of one ceramic layer is equal to 70 µm (after shrinkage in Z direction). Three layers of LTTC foils were used under and above a strip which is shown in Fig. 2.

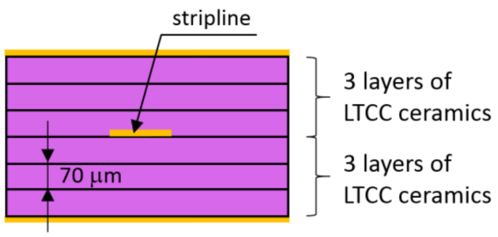

Fig. 2. Cross-section of the designed multilayered stripline

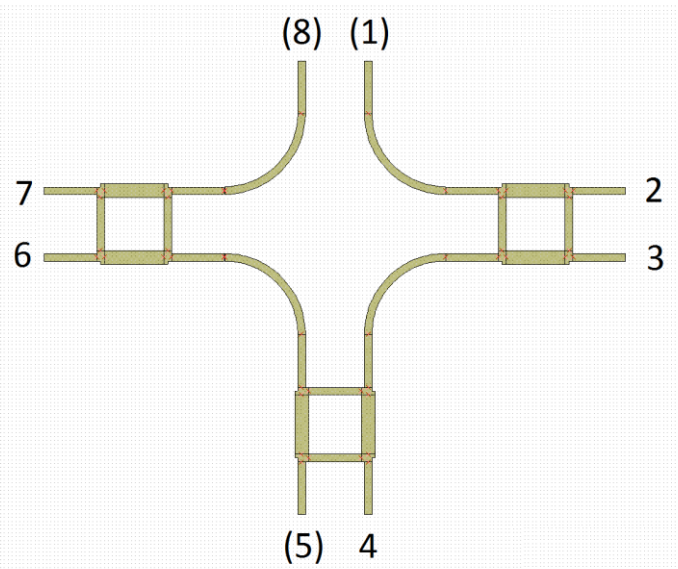

Fig. 3. Layout of stripline six-port

In NI AWR Design Environment there were not such elements as power dividers for stripline, so in Fig. 3 there are only three quadrature 3 dB couplers, without power divider which can be added to ports (1) and (8). For this reason magnitudes of S-parameters presented in Table I refer to simultaneous excitation of ports (1) and (8). As a consequence, $|S_{21}|$ and $|S_{31}|$ (same as $|S_{68}|$ and $|S_{78}|$) are approximately 3 dB higher than in the structure with power divider. Phase difference between ports 2 and 3 equals to 89.8°. Other phase differences are also close to nominal values for six-port device.

Table I
S-Parameters at 24 GHz for the Six-Port from Fig. 3

Parameter	Value
$\|S_{11}\|$ [dB]	-37.82
$\|S_{21}\|$, $\|S_{78}\|$ [dB]	-3.23
$\|S_{31}\|$, $\|S_{68}\|$ [dB]	-3.26
$\|S_{41}\|$ [dB]	-46.45
arg(S_{21}) – arg(S_{31}) [°]	89.80

In the next step microstrip lines were added to stripline couplers in order to mount connectors to them (Fig. 4). Cross-section of microstrip structure is shown in Fig. 5.

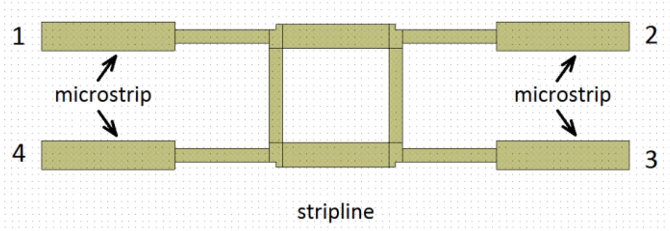

Fig. 4. Layout of stripline coupler with added microstrip lines

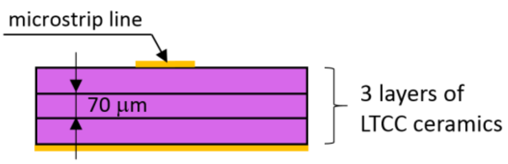

Fig. 5. Cross-section of the designed multilayered microstrip

Table II
S-Parameters at 24 GHz for Two Stripline Couplers – with and without Additional Microstrip Lines

Parameter	Value (stripline coupler)	Value (stripline coupler with microstrip lines)
$\|S_{11}\|$ [dB]	-36.06	-36.66
$\|S_{21}\|$ [dB]	-3.13	-3.19
$\|S_{31}\|$ [dB]	-3.16	-3.22
$\|S_{41}\|$ [dB]	-43.15	-42.37
arg(S_{21}) – arg(S_{31}) [°]	89.80	89.80

Results for the coupler, with attached microstrip lines (Fig. 4) are comparable to the results for the stripline coupler without additional lines and they are presented in Table II. In this model two types of transmission lines are connected directly. It causes discontinuity in upper dielectric layer with upper ground plane in case of stripline. The influence of this discontinuity is not observed in the results of simulations. It is associated with simplified models of circuit simulator which do not take into account effects such as radiation, coupling and boundaries of a structure. Moreover, in this kind of simulators infinite ground plane is assumed. Hence, it was decided to carry out simulations in full-wave electromagnetic simulator FEKO.

IV. Design of Six-Port Device by Using of Full-Wave Simulator

The main issue in this part of paper is the transition between stripline and microstrip. The usage of two types of transmission lines causes some difficulties. Direct transition is not well matched and demonstrates significant insertion loss mainly related to radiation. Return signal current is shared between upper and lower dielectric layers but upper layer abruptly ends. Return current can not follow its path and it should be corrected [8]. Typically, in such cases ground vias are used. However, there are a lot of problems with fabricating vias in LTCC ceramics. For this reason, in this project metal walls were used instead of vias.

While filling via holes with a paste comprising metal particles, at the bottom of a via hole an air bubble can remain. It may result that there is no connection between lower and upper metal layers [9]. To resolve this problem the vacuum can be used to suck the metal paste into the via hole. However, for mm-wave structures it is not easy, because they often require additional layer, e.g., alumina plate, to make whole structure more durable. Additionally, placing green tapes on alumina plate allows to achieve flat and smooth surfaces after sintering. Unfortunately, it is hard to drill small holes in it. There are also some other problems with making vias. After co-firing vias can have sharpened edges or can be filled with too small amount of metal paste. Therefore, it affects performance of a device [10]. For these reasons using metal walls to create vertical interconnections between layers seems to be better than using vias (Fig. 6). Thanks to such design better matching and lower insertion losses could be obtained.

A. Transition between microstrip and stripline

Direct transition between microstrip and stripline radiates and is not well matched as it was mentioned previously. In Fig. 7 its scattering parameters are shown. In simulations it was assumed that metal layers are made of perfect electric conductor (PEC) of zero thickness.

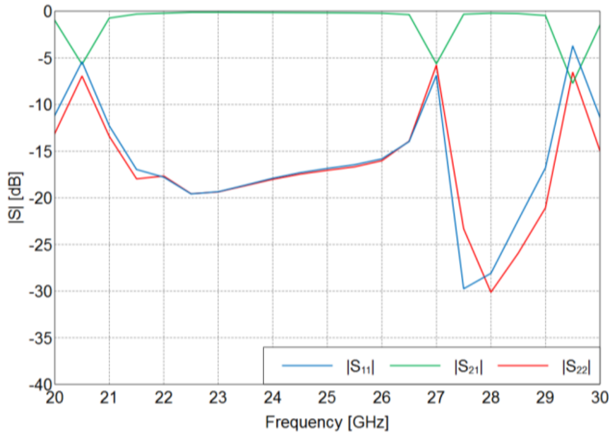

Fig. 7. Magnitudes of S-parameters for direct transition between microstrip and stripline

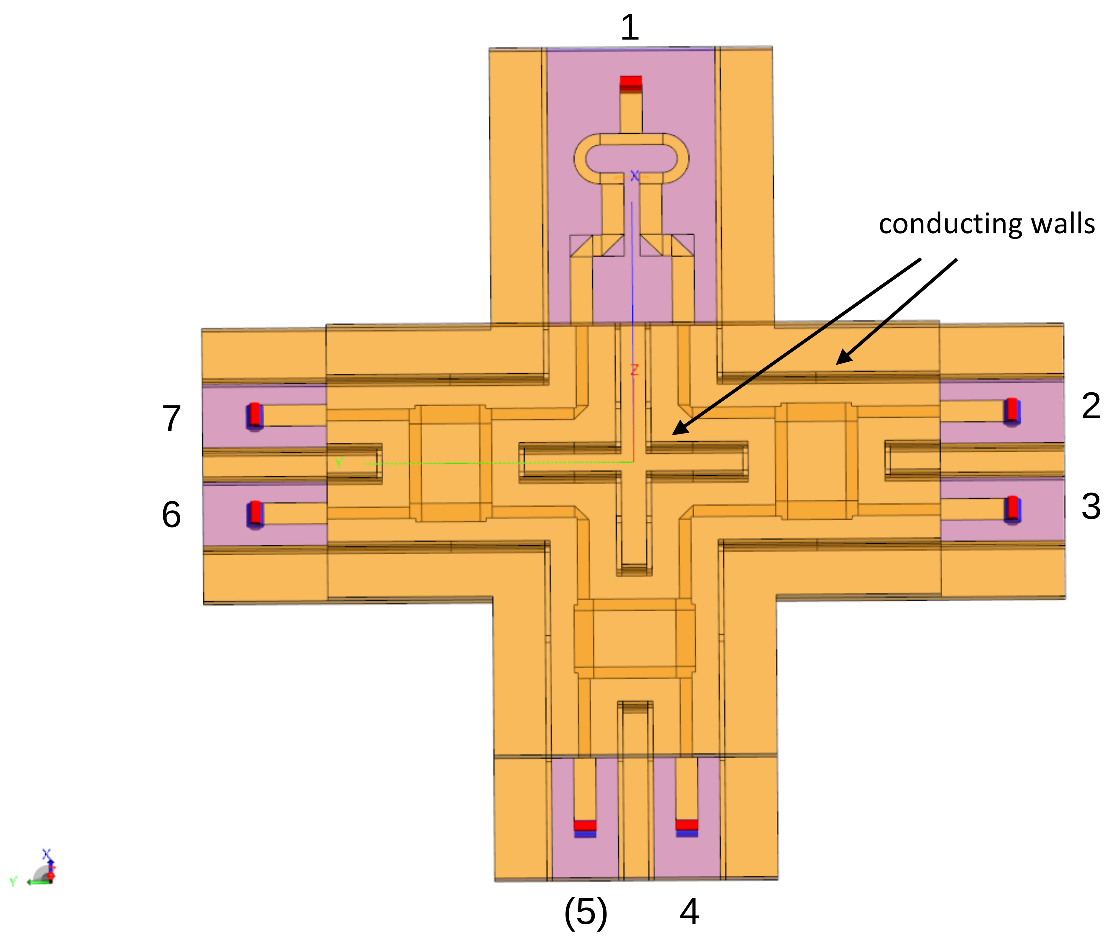

Fig. 6. Model of designed six-port

To achieve required value of reflection coefficient appropriate changes have to be applied to direct transition. Along the lines, on both sides, equidistant vias were added. Further, dielectric layer in the middle of the structure was coated by a metal sheet which is shown in Fig. 8. In addition, dielectric outside metal walls was also coated. Proposed solutions provide satisfying values of reflection and transmission coefficients (Fig. 9).

Due to the problems with fabricating vias in LTCC structures which were described previously, vias were substituted by metal walls without changing other parameters (Fig. 10). Thanks to that $|S_{11}|$ have lower value in whole 24 GHz band (Fig. 11).

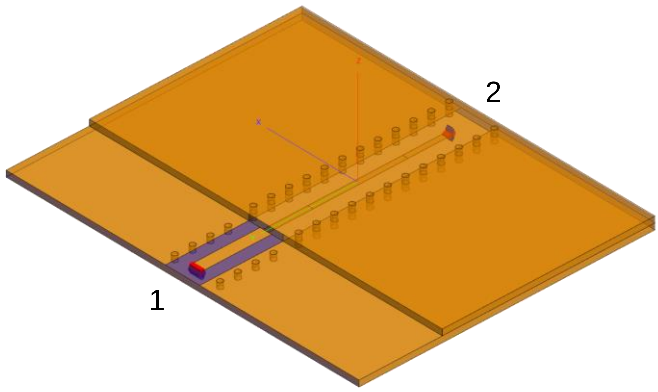

Fig. 8. Model of optimized transition between microstrip and stripline (with vias)

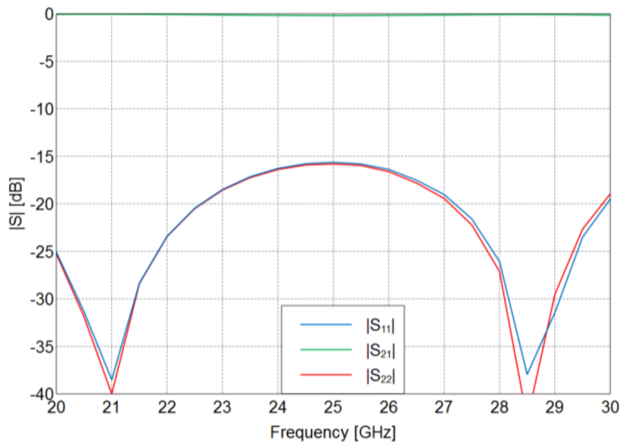

Fig. 9. Magnitudes of S-parameters for transition between microstrip and stripline with vias

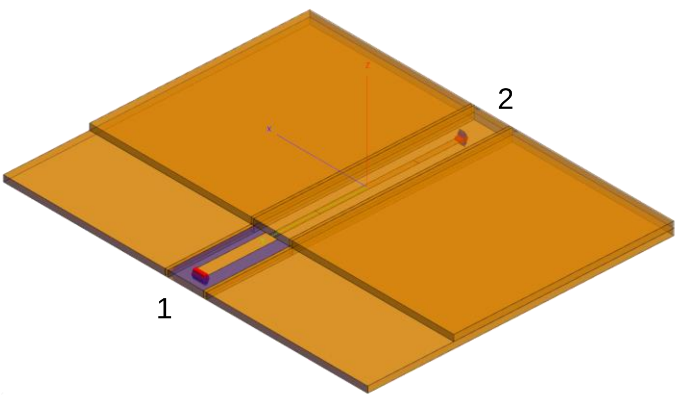

Fig. 10. Model of optimized transition between microstrip and stripline (with metal walls)

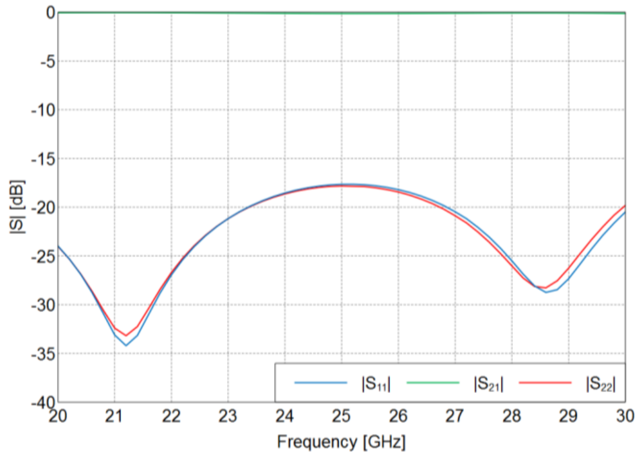

Fig. 11. Magnitudes of S-parameters for transition between microstrip and stripline with metal walls

B. *Design of a quadrature coupler*

The model of the stripline coupler was complemented with designed transitions between microstrip and stripline (Fig. 12). Modifications described in section A were also applied. Along the coupler's arms conducting walls were inserted. However, as opposed to the model of transition, conductor sheets between dielectric layers in stripline area were removed. Due to the usage of metal walls it was not necessary. Stripline and microstrip line widths of modified structure were optimized and satisfactory results were achieved. Values of reflection coefficient, transmission and isolation are presented in Fig. 13.

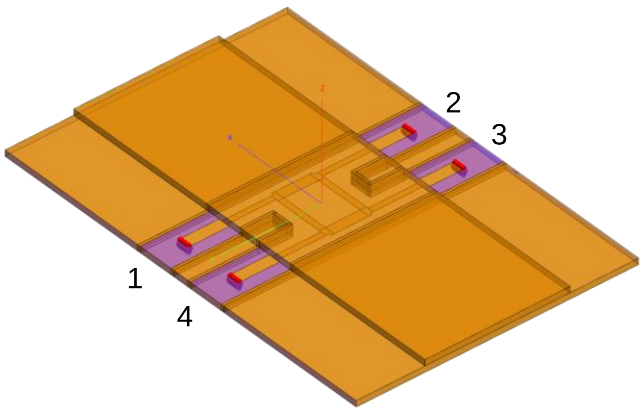

Fig. 12. Model of designed quadrature coupler

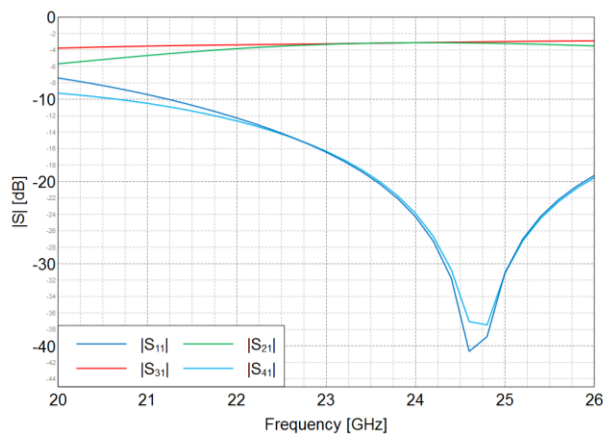

Fig. 13. Magnitudes of S-parameters for optimized coupler with metal walls

Fig. 14 and Fig. 15 show electric field distribution 100 μm above the inner conductor of stripline at 24 GHz for the coupler without and with metal walls, respectively. In the first case electric field is widely dispersed over a large area and radiation from the structure can be observed. This phenomenon adversely affects performance of the coupler as it was described in section A. The usage of conducting walls eliminates these unfavourable effects and electric field is concentrated near transmission lines (Fig. 15).

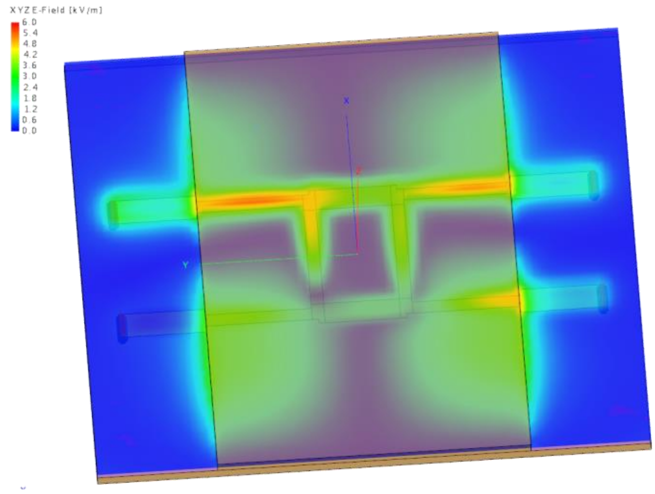

Fig. 14. Electric field distribution for coupler without metal walls

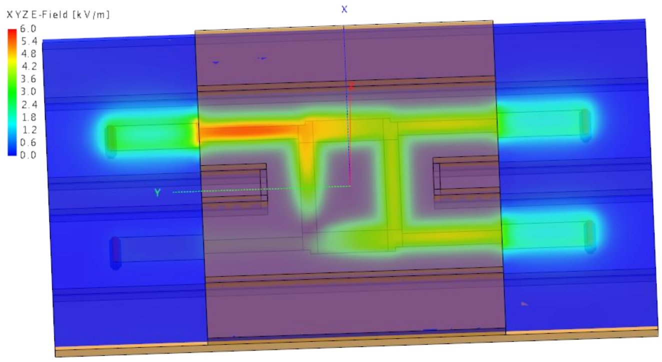

Fig. 15. Electric field distribution for coupler with metal walls

C. *Design of a Wilkinson power divider*

The Wilkinson power divider was designed using microstrip lines. Thanks to that it would be simpler for fabrication and mounting discrete components. Simulation model of designed power divider is shown in Fig. 16. Appropriate width of the gap between arms of the divider was selected in order to mount a 0201 chip resistor.

Presented power divider features satisfying simulation results. Its characteristics are shown in Fig. 17. S-parameters at 24 GHz are presented in Table III. Transmission from input port to output ports is good and equals -3.08 dB. Reflection coefficients for all ports are below -14 dB. Isolation between output ports is equal to approximately -17 dB.

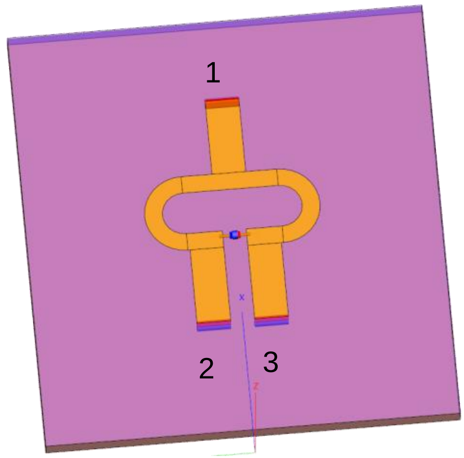

Fig. 16. Model of Wilkinson power divider

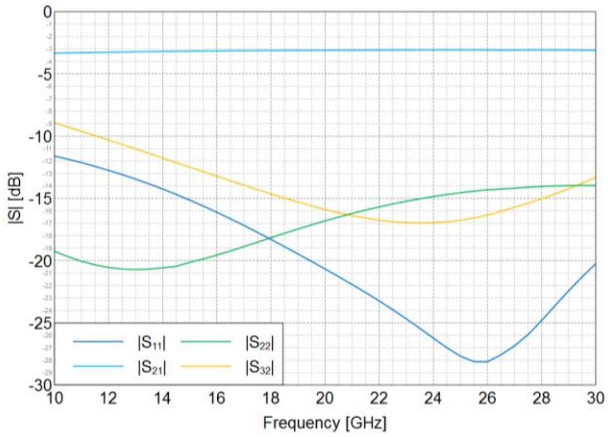

Fig. 17. Magnitudes of S-parameters for Wilkinson power divider

TABLE III
S-PARAMETERS FOR WILKINSON POWER DIVIDER AT 24 GHZ

Parameter	Value
$\|S_{11}\|$ [dB]	-26.24
$\|S_{22}\|$, $\|S_{33}\|$ [dB]	-14.86
$\|S_{21}\|$, $\|S_{31}\|$ [dB]	-3.08
$\|S_{32}\|$ [dB]	-16.96

D. *Design of the six-port*

Model of six-port shown in Fig. 6 is composed of three quadrature couplers, Wilkinson power divider and additional microstrip lines. This model of the structure was simulated twice. Firstly, when all conducting layers are made of perfect electric conductor (PEC) of zero thickness (Fig. 6). Secondly, for stripline and microstrip lines which have conductivity $\sigma=10^7$ S/m and 5 μm thickness. These lines were denoted by green colour in Fig. 18. The six-port has two input ports which were numbered as 1 and 4. Ports 2, 3, 6 and 7 are outputs of the structure. A port 5 is omitted in simulation results because it is connected to a matched load. All figures and tables presented below are related to the second case – with lossy conductor.

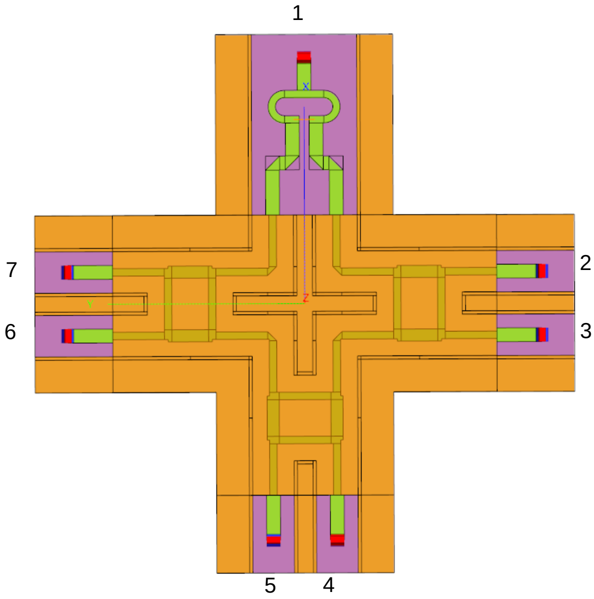

Fig. 18. Model of designed six-port with lossy lines (denoted by green colour)

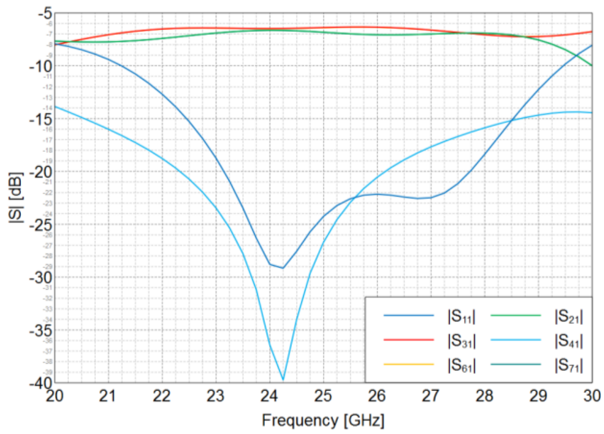

Fig. 19. Magnitudes of S-parameters for six-port for excitation of port 1

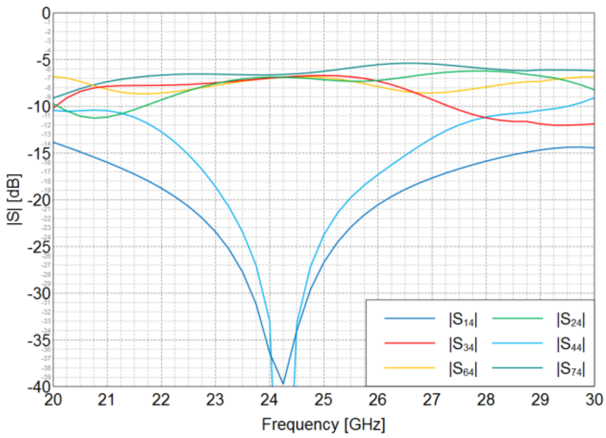

Fig. 20. Magnitudes of S-parameters of six-port for excitation of port 4

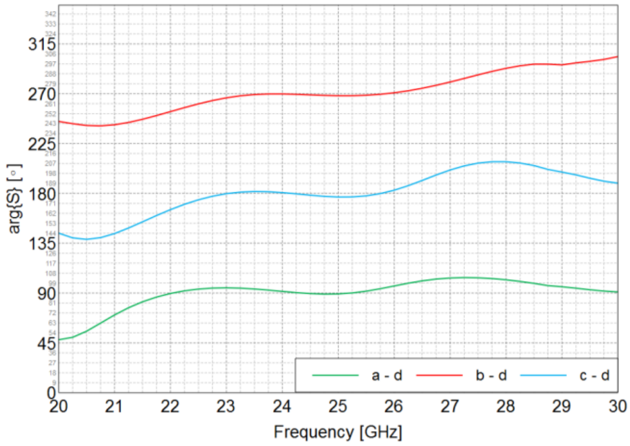

Fig. 21. Phase differences at the outputs normalized to phase of the signal at port 7 in the case of simultaneous excitation

After final optimization of the line widths satisfactory results in the whole 24 GHz band were obtained. Fig. 19 and Fig. 20 present S-parameters when port 1 and port 4 are excited, respectively. It can be seen that matching, isolation between input ports and transmission to output ports are very good. The values of these parameters for the lowest and the highest frequencies of the given band are gathered in Table IV and Table V. Phase differences at the outputs in the case of simultaneous excitation of input ports are presented in Fig. 21 and Table VI. The results are normalized to phase of the signal at port 7. The letter designators are assigned to the following ports: a – 2, b – 3, c – 6, d – 7. Obtained phase shifts are very close to 90°, 180° and 270°.

TABLE IV
S-PARAMETERS OF SIX-PORT AT 24 AND 24.25 GHZ FOR EXCITATION OF PORT 1

Parameter	Value at 24 GHz	Value at 24.25 GHz
$\|S_{11}\|$ [dB]	-28.79	-29.15
$\|S_{21}\|$ [dB]	-6.64	-6.65
$\|S_{31}\|$ [dB]	-6.48	-6.47
$\|S_{41}\|$ [dB]	-36.46	-39.73
$\|S_{61}\|$ [dB]	-6.50	-6.49
$\|S_{71}\|$ [dB]	-6.65	-6.66

TABLE V
S-PARAMETERS OF SIX-PORT AT 24 AND 24.25 GHZ FOR EXCITATION OF PORT 4

Parameter	Value at 24 GHz	Value at 24.25 GHz
$\|S_{14}\|$ [dB]	-36.46	-39.74
$\|S_{24}\|$ [dB]	-6.87	-6.87
$\|S_{34}\|$ [dB]	-6.98	-6.88
$\|S_{44}\|$ [dB]	-33.62	-67.40
$\|S_{64}\|$ [dB]	-6.98	-6.88
$\|S_{74}\|$ [dB]	-6.63	-6.59

TABLE VI
PHASE DIFFERENCES AT THE OUTPUTS NORMALIZED TO PHASE OF THE SIGNAL AT PORT 7 IN THE CASE OF SIMULTANEOUS EXCITATION

Parameter	Value at 24 GHz	Value at 24.25 GHz
a – d [°]	91.50	90.36
b – d [°]	269.80	269.40
c – d [°]	180.70	179.60
d – d [°]	0	0

Compared to the six-port with perfect electric conductor, transmission coefficients between port 1 and output ports were decreased by less than 0.5 dB. In the case of port 4 decrease is not higher than 0.6 dB. Phase shifts do not differ significantly.

V. CONCLUSION

The Low Temperature Cofired Ceramic technology has been significantly improved in the last few years. It can meet requirements of fabrication accuracy and resolution which are crucial for mm-wave devices. LTCC materials have also very good electrical and mechanical properties, temperature stability and high reliability. In this paper design of LTCC six-port device for 24 GHz band was presented. Due to relatively large area of the structure properties of LTCC are very important. The proposed six-port is composed of stripline quadrature couplers and microstrip power divider. The use of stripline provides possibility of making three dimensional structures minimizing overall surface of a device. Moreover, microstrip facilitates mounting connectors and discrete components.

The model takes into account limitations of the LTCC technology. It means that appropriate modifications were applied. Especially, metal walls instead of standard vias were used. The results of electromagnetic simulations proved correctness of proposed solutions. Designed six-port is well matched, isolation between input ports is relatively high and phase differences are close to ideal values.

REFERENCES

[1] L. Golonka, “Technology and Applications of Low Temperature Co-Fired Ceramic (LTCC) Based Sensors and Microsystems,” Bulletin of the Polish Academy of Sciences: Technical Sciences, vol. 54, no. 2, pp. 221-231, 2006
[2] J. Sobolewski and P. R. Bajurko, “Design of LTCC patch antenna for increased bandwidth and reduced susceptibility to fabrication process inaccuracies,” in 2018 22nd International Microwave and Radar Conference (MIKON), Poznan, 2018, pp. 218-221. DOI: 10.23919/MIKON.2018.8405182.
[3] T. Jiang, “Six-port technology for millimeter-wave MIMO systems,” Masters thesis, École Polytechnique de Montréal, 2014.
[4] A. Koelpin, et al., “Six-Port Based Interferometry for Precise Radar and Sensing Applications,” Sensors (Basel), vol. 16, no 10, Sep. 2016. DOI: 10.3390/s16101556
[5] A. Koelpin, G. Vinci, B. Laemmle, D. Kissinger and R. Weigel, “The Six-Port in Modern Society,” in IEEE Microwave Magazine, vol. 11, no. 7, pp. 35-43, Dec. 2010. DOI: 10.1109/MMM.2010.938584.
[6] В. И. Гвоздев, Е. И. Нефёдов, “Объемные интегральные схемы СВЧ,”, Москва, Наука, 1985.
[7] P. R. Bajurko, “Millimeter wave permittivity and loss tangent measurements of LTCC materials,” 2016 21st International Conference on Microwave, Radar and Wireless Communications (MIKON), Krakow, 2016, pp. 1-4. DOI: 10.1109/MIKON.2016.7492104
[8] H. W Johnson, M Graham, “High-Speed Digital Design, A Handbook of Black Magic,” 1st ed., Prentice Hall, 1993
[9] X. Q. He, X. Ma and Y. Zhang, “Elimination of opens failure between via holes and traces in LTCC multilayer substrate by coherent shrinkage,” Proceedings of the 2001 8th International Symposium on the Physical and Failure Analysis of Integrated Circuits. IPFA 2001, Singapore, 2001, pp. 138-141. DOI: 10.1109/IPFA.2001.941472
[10] Y. Yashchyshyn et al., “Experience in developing LTCC technologies for mm-Wave antennas,” 2017 11th European Conference on Antennas and Propagation (EUCAP), Paris, 2017, pp. 1306-1310. DOI: 10.23919/EuCAP.2017.7928083